



## CLINICAL ARTICLE

# Differential Diagnosis of Mimicking Tumor Discs Using Coronal Magnetic Resonance Imaging of Three-Dimensional Fast-Field Echo with Water-Selective Excitation: A Single Center Retrospective Study

Jinghong Yuan, MS<sup>1</sup> , Zhi Du, MS<sup>1</sup>, Zhiwen Wu, MS<sup>1</sup>, Jianhua Yin, MD<sup>2</sup>, Bingxue Cheng, MS<sup>2</sup>, Xi Xiong, MS<sup>3</sup>, Sikuan Zheng, MS<sup>1</sup>, Xijuan Liu, MD<sup>4</sup>, Jingyu Jia, ME<sup>1</sup>, Xigao Cheng, MD<sup>1</sup> 

Department of <sup>1</sup>Orthopaedics, <sup>2</sup>Radiology and <sup>4</sup>Paediatrics, The Second Affiliated Hospital of Nanchang University, Nanchang and <sup>3</sup>Department of Orthopaedics, Fengcheng People's Hospital, Fengcheng, China

## Abstract

**Objective:** As disc fragment completely loses contact with the parent disc and can migrate in all directions of the epidural space, making it appear similar to schwannoma, it is fairly difficult to make a definitive diagnosis for mimicking tumor discs. The aim of this research is to differentially diagnose mimicking tumor discs and schwannomas using coronal magnetic resonance imaging (MRI) of three-dimensional fast-field echo with water-selective excitation (CMRI).

**Methods:** Among 76 patients (38 men and 38 women; mean age,  $52.88 \pm 15.80$  [range, 18–78 years]) who were retrospectively examined in this study, 38 were primarily diagnosed with schwannomas and pathologically diagnosed with mimicking tumor discs after surgery, and 38 were primarily diagnosed with neurogenic tumors and pathologically diagnosed with schwannomas after surgery. Open surgery was performed in all the patients between March 2016 and April 2020. The preliminary diagnosis of all patients was considered an intraspinal tumor based on conventional two-dimensional MRI sequences. After open surgery, the final diagnosis was confirmed to mimic a tumor disc or schwannoma based on postoperative pathology reports. The sensitivity, specificity, and reliability of CMRI and conventional MRI for identifying mimicking tumor discs and schwannomas were compared. Chi-square and McNemar tests were used for statistical analyses.

**Results:** Symptoms were considerably relieved in all the patients after surgery. Seven patients had grade 1 extensor digitorum longus, triceps surae, or quadriceps femoris muscle strength prior to surgery. No nerve root injury was observed in any of the patients. CMRI showed significantly higher sensitivity (94.74%) and specificity (94.74%) than conventional MRI (71.05% and 92.11%, respectively;  $p = 0.012 < 0.05$ , and  $p = 1 > 0.05$ , respectively) for differential identification between mimicking tumor discs and schwannomas. Moreover, CMRI showed a higher reliability (kappa value = 0.787) than conventional MRI (kappa value = 0.374).

**Conclusions:** CMRI is a better non-invasive technology for the identification of intraspinal lesions, especially for differentiating between mimicking tumor discs and schwannomas.

**Key words:** magnetic resonance imaging; mimicking tumor discs; reliability; schwannoma; sensitivity

**Address for correspondence** Jingyu Jia and Xigao Cheng, Department of Orthopedics, The Second Affiliated Hospital of Nanchang University, 1 Minde Road, Donghu District, Nanchang, Jiangxi 330006, P.R. China; Email: [jia-jingyu@163.com](mailto:jia-jingyu@163.com) (J. J.) and Email: [228206846@qq.com](mailto:228206846@qq.com) (X. C.)

Received 23 April 2021; accepted 25 July 2022

## Introduction

Disc sequestration is defined as a perforation of the fibrous ring and posterior longitudinal ligament, and fragment migration to the epidural space<sup>1</sup> accounts for 28.6% of all disc herniations<sup>2</sup>. The fragment completely loses contact with the parent disc and can migrate in all directions of the epidural space, for example superiorly, inferiorly, posteriorly, laterally, and intradurally. In some rare cases, the appearance of disc sequestration on magnetic resonance imaging (MRI) is similar to that of epidural tumors<sup>3-5</sup>. Therefore, disc sequestration is sometimes misdiagnosed as a tumor, such as meningioma or neurinoma. Emamian<sup>4</sup> named this type of disc sequestration a mimicking tumor disc for the first time in 1993. Since then, mimicking tumor discs have been reported many times and have become a challenge in terms of clinical diagnosis. Because of the difficulty in making a definitive diagnosis of mimicking tumor discs using computed tomography (CT), MRI, and gadolinium-enhanced (Gd) MRI before surgery, open surgery was performed in almost all previously reported cases<sup>1,5-24</sup>.

MRI is considered the most appropriate non-invasive modality for confirming the presence of lumbar disc herniation<sup>25</sup>. Although several studies have found that disc fragments can demonstrate a characteristic Gd-MRI appearance, such as peripheral rim enhancement, and can differentiate mimicking tumor discs from metastatic tumors, hematomas, and meningiomas, the characteristic appearance is not helpful for differentiating mimicking tumor discs from neurinomas. In 2017, Takano *et al.* observed a mass located posterolaterally in the dural sac in a 78-year-old man using MRI. The mass was a posterior epidural migration of lumbar disc fragments, malignancy, spontaneous hematoma, or epidural abscess<sup>22</sup>. To confirm the diagnosis, L3/4 discography and disco-CT were performed. Subsequently, the mass was successfully identified as mimicking a tumor disc using discography and disco-CT because of contrast medium leakage into the posterior dural space. Intraoperatively, the lesion was verified as a herniated disc fragment. Although discography is helpful for the diagnosis of mimicking tumor disc herniation, it is an invasive technique, and complications, such as nerve root injury and infection, are inevitable.

To avoid these disadvantages, coronal MRI of three-dimensional (3D) fast-field echo with water-selective excitation (CMRI) is considered a non-invasive and reliable novel technology<sup>26-29</sup>. Byun *et al.* and Shen *et al.* confirmed that CMRI can show the whole length of the nerve root from the origin of the nerve root to the extraforaminal region; the 3D space between the herniated disc and nerve root can also be shown after CMR images are reconstructed without invasive examination<sup>26,27</sup>. Because of its non-invasive and highly reliable technical features, CMRI is significantly superior to conventional MRI and discography. A previous study indicated that mimicking tumor discs were differentiated from neurinomas in two cases in 2018<sup>29</sup>. However, to date, the sensitivity, specificity, and reliability of CMRI for the diagnosis of

mimicking tumor discs have not been addressed, and the characteristics of mimicking tumor discs on CMRI have not been analyzed. Therefore, this study aimed to (i) compare the reliability of conventional MRI and CMRI for identifying mimicking tumor discs, (ii) compare the sensitivity and specificity of conventional MRI and CMRI for identifying mimicking tumor discs, and (iii) determine the characteristics of mimicking tumor discs on CMRI.

## Methods

### Ethics Statement

This single-blind retrospective study was approved by the medical ethics committee of our institution (Review 2016, No. 001). Informed consent was obtained from all patients.

### Study Design and Population

Medical records and MRIs of patients who were primarily diagnosed with schwannomas, and pathologically diagnosed with mimicking tumor discs after surgical procedures, and those who were primarily diagnosed with neurogenic tumors, and pathologically diagnosed with schwannomas after surgical procedures were retrospectively reviewed between March 2016 and April 2020 using the PACS system of our institution. Next, according to the number of postoperative cases pathologically diagnosed mimicking tumor discs, the same number of postoperative cases of pathologically diagnosed schwannomas were randomly selected.

The inclusion criteria for patients mimicking tumor discs were as follows: (i) a preliminary diagnosis of intraspinal tumor based on conventional two-dimensional MRI sequences; (ii) definite diagnosis confirmed using Gd-MRI and CMRI; (iii) 3D images reconstructed using maximum-intensity projection and a volume-rendering technique according to a previous report; and iv) open surgery was conducted, and the final diagnosis was confirmed as a mimicking tumor disc or schwannoma based on postoperative pathology reports.

The exclusion criteria were as follows: a history of (i) lumbar spine surgery, or (ii) lumbar spondylolisthesis, lumbar spinal stenosis, or lumbar scoliosis. Patients mimicking tumor discs and schwannomas were examined to calculate the sensitivity of conventional MRI and CMRI for identifying mimicking tumor discs and schwannomas.

### Surgical Procedures

The patients were placed in the prone position under general anesthesia on a radiolucent operating table. The skin and subcutaneous tissues were incised on the midline along the spinous processes, towels were attached to the skin edges with clips, or an adhesive plastic drape was used. The deep fascia and supraspinous ligament were divided in line with a skin incision. Using high-frequency electrosurgical equipment, the supraspinous ligament was removed from the tip of the spine. This procedure was repeated until the desired number of vertebrae was exposed. For surgeries requiring

exposure of both sides of the spine, the same technique was used on each side. This approach exposed the spinous processes and the medial part of the laminae. The exposure could be increased if desired by performing further subperiosteal reflection along the laminae, exposing the posterior surface of the laminae and articular facets. The lumbar spine was fixed with polyaxial pedicle screws and fixation was confirmed using a C-arm machine. The spinous process and lamina were removed using an ultrasonic osteotome and laminar rongeur, exposing the dura mater and nerve roots. A surgical microscope (M525 F50; Leica Microsystems, Wetzlar, Germany) was used to visualize tumor discs or schwannomas.

### Coronal MRI of Three-Dimensional Fast-Field Echo with Water-Selective Excitation

The CMRI scanning parameters were consistent with those used in previous studies<sup>28,29</sup>. Sequence development was performed using a 3.0-T whole-body scanner (GE Medical Systems, Chicago, IL) with a spine coil. Conventional axial T2 fast spin echo (4180/102) (repetition time ms/echo time ms), sagittal T2 fast spin echo (2200/120), and sagittal T1 fast spin echo (460/20) were used to acquire the original images. The 3D coronal CUBE-MRN sequence was then acquired using the following acquisition parameters for a 1-mm-thick section without an overlapping section gap: repetition time, 2000 ms; echo time, 32 ms; 352 × 256 matrix; 32-cm field of view; 20° flip angle; and two signal intensity acquisitions. Original coronal fast spin echo images were acquired. The imaging plane was set parallel to the longitudinal axis of the lumbar spinal cord and centered on the level of the L3 vertebral body. The coronal image was reconstructed using maximum-intensity projection and the volume-rendering technique in ADW software (4.6 version; GE Medical Systems, Chicago, IL).

### Analysis and Evaluation

Three experts were involved in the study, including two orthopaedic surgeons (JJ and XC) and one radiologist (JY). Conventional MR and CMR images were evaluated by three experts, and the reliability, sensitivity, and specificity for identifying mimicking tumor discs and schwannomas were recorded.

### Statistical Analysis

Statistical analysis was performed using SPSS version 25.0 for Windows (IBM Corp., Armonk, NY). Interobserver agreement was evaluated using kappa analysis according to a previous study<sup>30</sup>. A kappa value of 0.00–0.20 was considered as slight agreement, 0.21–0.40 as fair agreement, 0.41–0.60 as moderate agreement, 0.61–0.80 as substantial agreement, 0.81 to <1.00 as almost perfect agreement, and 1.00 as perfect agreement. Chi-square and McNemar tests were used to analyze the sensitivity and specificity for identifying mimicking tumor discs and schwannomas between conventional MRI and CMRI. *p*-values <0.05 were considered statistically significant.

### Results

#### Baseline Characteristics

From March 2016 to April 2020, 38 patients who were primarily diagnosed with schwannomas and pathologically diagnosed with mimicking tumor discs after surgical procedures, and 108 patients who were primarily diagnosed with neurogenic tumors and pathologically diagnosed with schwannomas after surgical procedures fulfilled the inclusion criteria and were retrospectively examined using data obtained using the PACS systems of our hospital. Subsequently, we randomly selected 38 of 108 patients with schwannomas for further analysis. Finally, 76 patients were included in the study: 38 patients mimicking tumor discs and 38 patients with schwannomas.

Open surgery was performed on all the patients. The mean age of the patients was  $52.88 \pm 15.80$  (range, 18–78) years old; there were 38 male patients with an average age of  $51.55 \pm 16.41$  (range, 19–78) years and 38 female patients with an average age of  $54.21 \pm 15.27$  (range, 18–76) years. Symptoms were significantly relieved in all patients after surgery.

### Coronal MRI of Three-Dimensional Fast-Field Echo with Water-Selective Excitation versus Conventional MRI

Conventional MRI showed fair agreement among the three observers, with kappa values ranging from 0.374 to 0.420 (Table 1 and Supplemental Tables S1–S3). However, CMRI showed substantial agreement between the three observers, with kappa values ranging from 0.638 to 0.787 (Table 1 and Supplemental Tables S4–S6). These findings indicate that CMRI has a higher reliability than MRI for identifying

**TABLE 1** CMRI showed a higher reliability on the identification of mimicking tumor discs than conventional MRI

Observer	MRI		CMRI	
	Kappa value	<i>p</i> Value	Kappa value	<i>p</i> Value
Jingyu Jia vs Xigao Cheng	0.374	0.019	0.787	<0.001
Jingyu Jia vs Jianhua Yin	0.420	0.006	0.638	<0.001
Xigao Cheng vs Jianhua Yin	0.393	0.015	0.787	<0.001



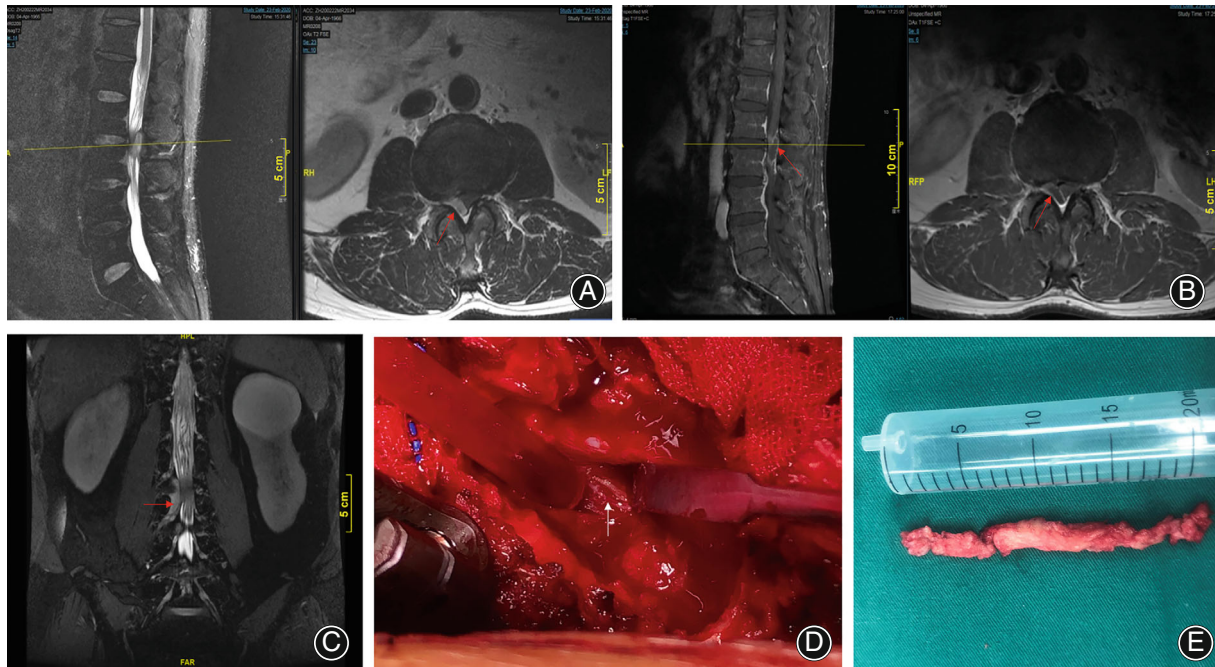


**Fig. 1** CMRI showed significantly higher sensitivity and specificity than conventional MRI for the identification of mimicking tumor disc. (A) Mimicking tumor disc was observed in the T2-weighted MRI (red arrow). (B) A characteristic peripheral rim enhancement was observed in the patients with mimicking tumor discs via Gd MRI (red arrow). (C) The mimicking disc mass (red arrow) showed a clear boundary with nerve root and dura via the evaluation of CMRI. Meanwhile, the signal intensity of the mass was uniform on CMRI. Unlike neurinoma, no annular lateral wall was observed via the evaluation of CMRI. (D) White arrow showed the rupture of posterior longitudinal ligament. (E) The mimicking disc mass was removed

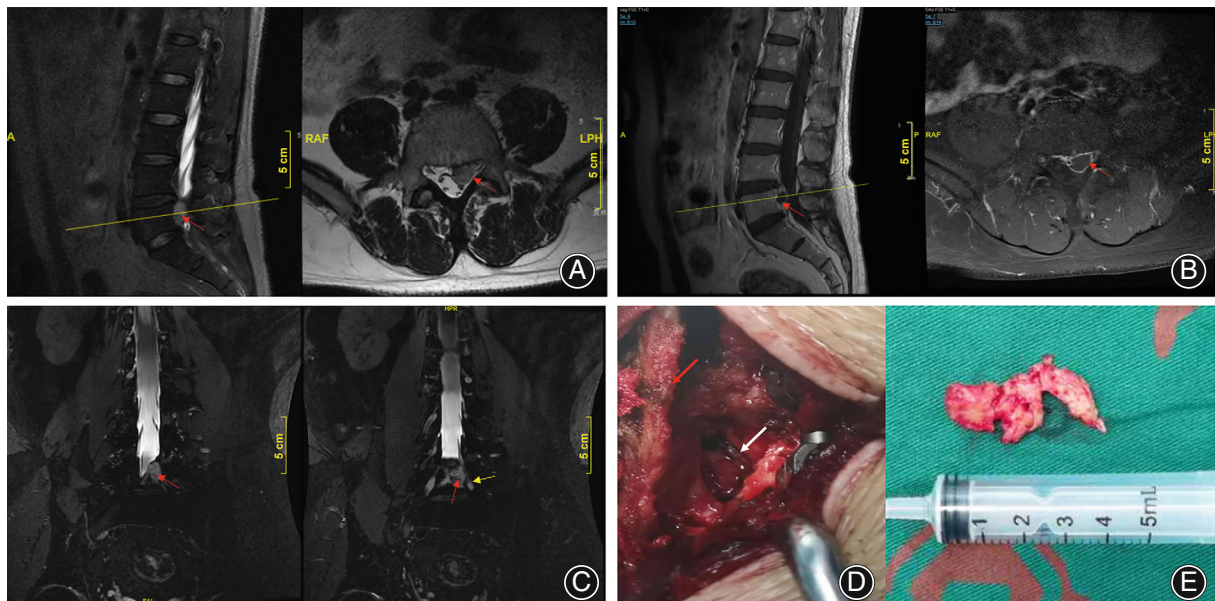


**Fig. 2** A characteristic peripheral rim enhancement was observed in the patients with mimicking tumor discs via Gd MRI. (A) Mimicking tumor disc was observed in the T2-weighted MRI (red arrow). (B) A characteristic peripheral rim enhancement was observed in the patients with mimicking tumor discs via Gd MRI (red arrow). (C) The mimicking disc mass (red arrow) showed a clear boundary with nerve root (yellow arrow) and dura via the evaluation of CMRI. (D) The vascular hyperplasia (white arrow) around mimicking tumor discs was observed during the operation. The spinous process was marked by red arrow. (E) The mimicking disc mass was removed

**TABLE 2** Comparison of MRI and CMRI in the diagnosis of schwannoma and mimicking tumor disc herniation

Observer	Schwannoma (n = 38)		Mimicking tumor discs (n = 38)	
	MRI, n (%)	CMRI, n (%)	MRI, n (%)	CMRI, n (%)
Xigao Cheng	35 (92.11)	36 (94.74)	27 (71.05)	36 (94.7)
Jingyu Jia	34 (89.47)	36 (94.74)	30 (78.95)	35 (92.1)
Jianhua Yin	35 (92.11)	36 (94.74)	25 (60.5)	34 (89.5)

mimicking tumor discs. More importantly, we observed that CMRI had significantly higher sensitivity and specificity (94.74% and 94.74%, respectively; Supplemental Table S7) than conventional MRI (71.05% and 92.11%, respectively;  $p = 0.012$  and  $p = 1 > 0.05$ , Supplemental Table S8) for identifying mimicking tumor discs (Figures 1 and 2, Table 2).

#### Imaging Characteristics of Mimicking Tumor Discs

In the present research, we have compared Gd MRI and CMRI radiographic images of mimicking tumor discs, schwannoma and intraspinal abscess, and a novel series of imaging features were observed. Although a ring-like

peripheral enhancement around the mass can be observed in mimicking tumor disc using Gd MRI (Figures 1B,C, 2B,C, 3B,C, 4B, and 5), it can also be detected in schwannoma and intraspinal abscess. This indicates that ring-like peripheral enhancement around the mass does not provide strong help in distinguishing mimicking tumor disc from schwannoma and intraspinal abscess. However, the imaging characteristics of mimicking tumor disc and schwannoma were different on CMRI. Firstly, there is a clear annular lateral wall around the mass of schwannoma, and the signal intensity of the wall is higher than the mass center on CMRI (Figures 3C and 5D-F), but no annular lateral wall was observed around the mass of mimicking tumor disc (Figures 1C and 2C). Then,

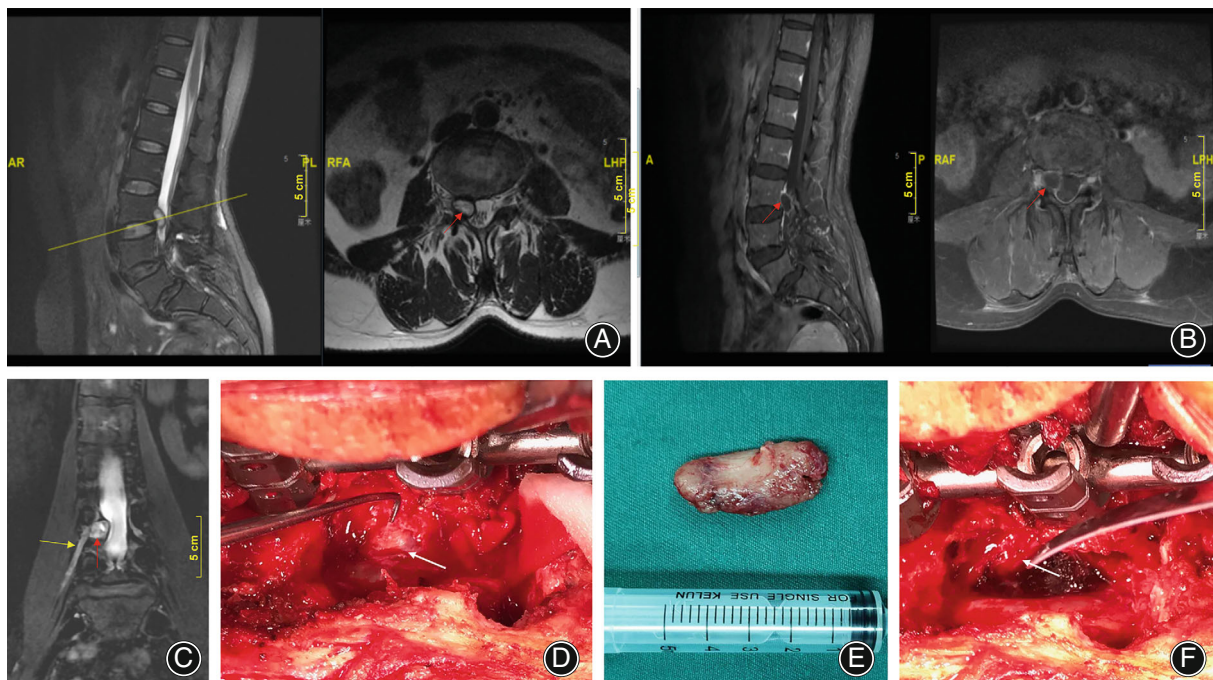


**Fig. 3** It seems not to be specific for the identification between mimicking tumor discs and neurinoma because neurinoma also present a ring-like peripheral enhancement via the evaluation of Gd MRI. (A) A mass (red arrow) was hidden behind the vertebral body of L3. (B) Like mimicking tumor discs, the mass also presented a ring-like peripheral enhancement on Gd MRI. (C) Though the mass demonstrated the clear boundary with dura, it is attached to the nerve root. Unlike mimicking tumor discs, the mass shows a clear annular lateral wall on CMRI, which cannot be observed in the mimicking tumor discs. The signal intensity of the lateral wall is higher than that of the center of the mass on CMRI and the signal intensity within the neurinoma is obvious nonuniform on CMRI. Additionally, spot-like hyperintense signals can also be observed within the mass. (D) Intraoperative observation confirmed that the mass is closely attached to the nerve root. (E) The mass was confirmed as neurinoma by postoperative pathology. (F) The nerve root (white arrow) was exposed after the neurinoma was completely resected



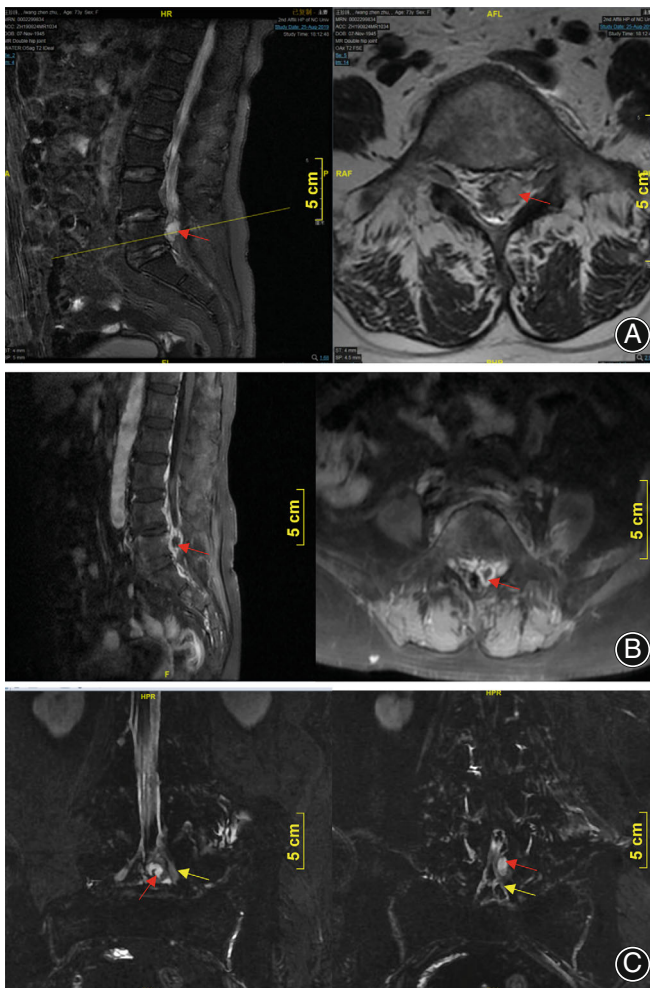


**Fig. 4** It seems not to be specific for the identification between mimicking tumor discs and neurinoma because intraspinal abscess also present a ring-like peripheral enhancement via the evaluation of Gd MRI. (A) A mass behind the vertebral body of L5 was observed in the T2-weighted MRI (red arrow). (B) Like mimicking tumor discs, the mass also presented a ring-like peripheral enhancement on Gd MRI. (C) Though the mass (red arrow) demonstrated the clear boundary with the nerve root (yellow arrow) and dura, the mass shows a uniform signal intensity, and the signal intensity of the mass was significantly higher than nerve root and dura, which is obviously different with the mimicking tumor discs and neurinoma

the signal intensity within the schwannoma is markedly non-uniform, and spot-like hyperintense signals can be observed within schwannoma (Figures 3C and 5D–F). However, the signal intensity on CMRI was uniform within the mimicking tumor disc (Figures 1C and 2C). Finally, the signal intensity of mimicking tumor discs is usually higher than their parent discs on MRI.

CMRI is also helpful for identifying mimicking tumor disc and intraspinal abscess. The mass of intraspinal abscess with a ring-like peripheral enhancement was similar to

mimicking tumor disc on Gd MRI (Figure 4B), and the annular lateral wall is unobserved on CMRI, as was mimicking tumor disc (Figure 4C). However, on CMRI, the signal intensity of the mass of intraspinal abscess is higher than the nerve root, which is the opposite of the mimicking tumor disc (Figure 4). Therefore, compared with Gd MRI, CMRI is a more reliable radiographic method for differential diagnosis of mimicking tumor disc, schwannoma, and intraspinal abscess.

### Complications

Seven patients had grade 1 extensor digitorum longus, triceps surae, or quadriceps femoris muscle strength before surgery. Five of the seven patients completely recovered 6 months after open surgery, and the other two patients acquired only some improvement in muscle strength of the lower limbs from grade 1 to grade 3 at 1 year after open surgery because of prolonged stress caused by the mimicking tumor disc on the nerve root. Cerebrospinal fluid leakage occurred in two patients owing to adhesion between the dura and discs. No nerve root injury was observed in any of the patients.

### Discussion

#### CT, Conventional MRI, and Gadolinium-Enhanced MRI of Mimicking Tumor Discs

In 2014, the North American Spine Society published evidence-based clinical guidelines for the diagnosis and treatment of lumbar disc herniation with radiculopathy in *The Spine Journal*<sup>25</sup>. The workgroup consensus statement is that if the symptoms and physical examination of patients are consistent with those of lumbar disc herniation with radiculopathy, MRI is considered an appropriate non-invasive test. Mimicking a tumor disc is a special type of disc herniation<sup>4</sup>. Since it was first reported, many scholars have reported cases of the disease one after another. Because of the difficulty in making a definitive diagnosis for mimicking tumor discs using CT, MRI, and Gd-MRI before surgery, open surgery was performed in almost all previously reported cases.<sup>1,5–23</sup> Although these patients showed a satisfactory therapeutic effect after open surgery, it does not seem to be the best strategy in some of them if surgeons can make a definite diagnosis of the mimicking tumor disc before surgery. Minimally invasive endoscopic surgery may be an alternative strategy that offers less damage, lower costs, and provides better therapeutic effects in some patients.

MRI is considered an effective tool for the diagnosis of intraspinal lesions. Therefore, they are often used to differentiate mimicking tumor discs from intraspinal abscesses, hematomas, meningiomas, metastases, and neurinomas. Several studies<sup>4,5,8,10,29,31</sup> have confirmed that mimicking tumor discs can demonstrate characteristic peripheral rim enhancement (i.e. a ring-like peripheral enhancement) on Gd-MRI, which can be due to the pathological changes of mimicking

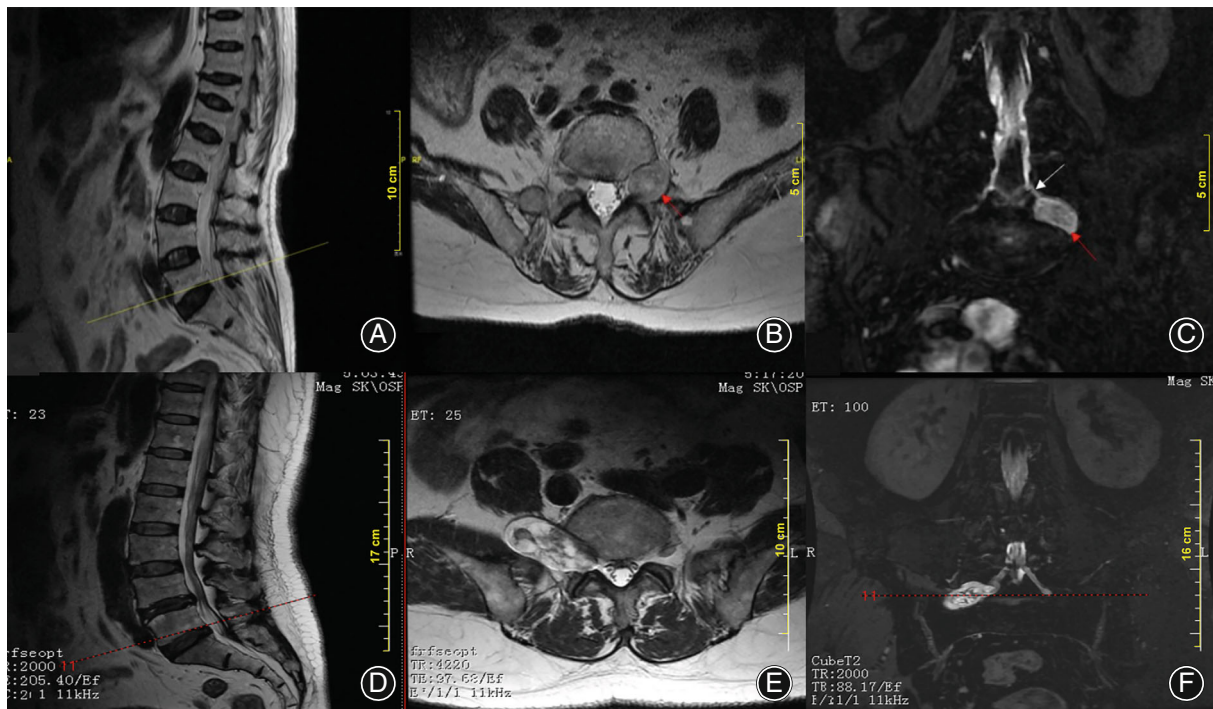


**Fig. 5** CMRI is a helpful tool for the differential diagnosis between mimicking tumor discs and neurinoma. (A–C) Unlike mimicking tumor discs, the neurinoma shows a clear annular lateral wall (red arrow) on CMRI, which cannot be observed in the mimicking tumor discs. The signal intensity of the lateral wall is higher than that of the center of the mass on CMRI. (D–F) The signal intensity within the neurinoma is obvious nonuniform on CMRI. Additionally, spot-like hyperintense signals can also be observed within the mass

tumor discs, such as vascular proliferation around intervertebral discs, inflammation, and vascular infiltration of the intervertebral disc<sup>6,7,29,31,32</sup>. Moreover, ring-like peripheral enhancement can be used to differentiate mimicking tumor discs from metastatic tumors, hematomas, and meningiomas. However, it is not specific because intraspinal abscesses and neurinomas also present with ring-like peripheral enhancement on Gd-MRI<sup>4,5,8–10</sup>.

#### **Coronal MRI of Three-Dimensional Fast-Field Echo with Water-Selective Excitation for the Diagnosis of Mimicking Tumor Discs**

In the present study, CMRI demonstrated higher sensitivity (CMRI, 93.74%; MRI, 71.05%), specificity (CMRI: 94.74%; MRI: 92.11%), and reliability (kappa value; CMRI: 0.638–0.787; MRI: 0.374–0.420) for identifying mimicking tumor discs than conventional MRI, which could be due to the characteristic appearance of mimicking tumor discs on CMRI.

#### **Imaging Characteristics of Coronal MRI of Three-Dimensional Fast-Field Echo with Water-Selective Excitation in Diagnosing Mimicking Tumor Discs**

In this study, characteristic peripheral rim enhancement (i.e. ring-like peripheral enhancement) was observed in 94.74% of patients mimicking tumor discs using Gd-MRI

(Figures 1 and 2). However, as in a previous report, this did not seem to be specific because intraspinal abscesses and neurinomas also present with a ring-like peripheral enhancement on Gd-MRI (Figures 3 and 4). CMRI is a helpful tool for making a differential diagnosis among mimicking tumor discs, intraspinal abscesses, and neurinomas (Figures 3–5). It was also vital to identify extraforaminal neuropathy and intradural tumors (Figures 6 and 7).

Similar to a previous report<sup>29</sup>, we found that the disc mass showed a clear boundary with the nerve root and dura on CMRI in all patients with mimicking tumor discs in the present study. In addition, we observed some new characteristic appearances on CMRI in patients' mimicking tumor discs. This characteristic information in this research is helpful in the differential diagnosis of mimicking tumor discs from schwannoma and intraspinal abscess using CMRI. First, using Gd-MRI, mimicking tumor discs and schwannoma were difficult to differentiate because of the similar imaging features; there was a ring-like peripheral enhancement around the mass. However, using CMRI, the differential diagnosis is clear, because only schwannomas show a clear annular lateral wall, and the signal intensity of the lateral wall is higher than that of the tumor center on CMRI. Moreover, the signal intensity within the schwannoma is non-uniform, and spot-like hyperintense signals can be observed

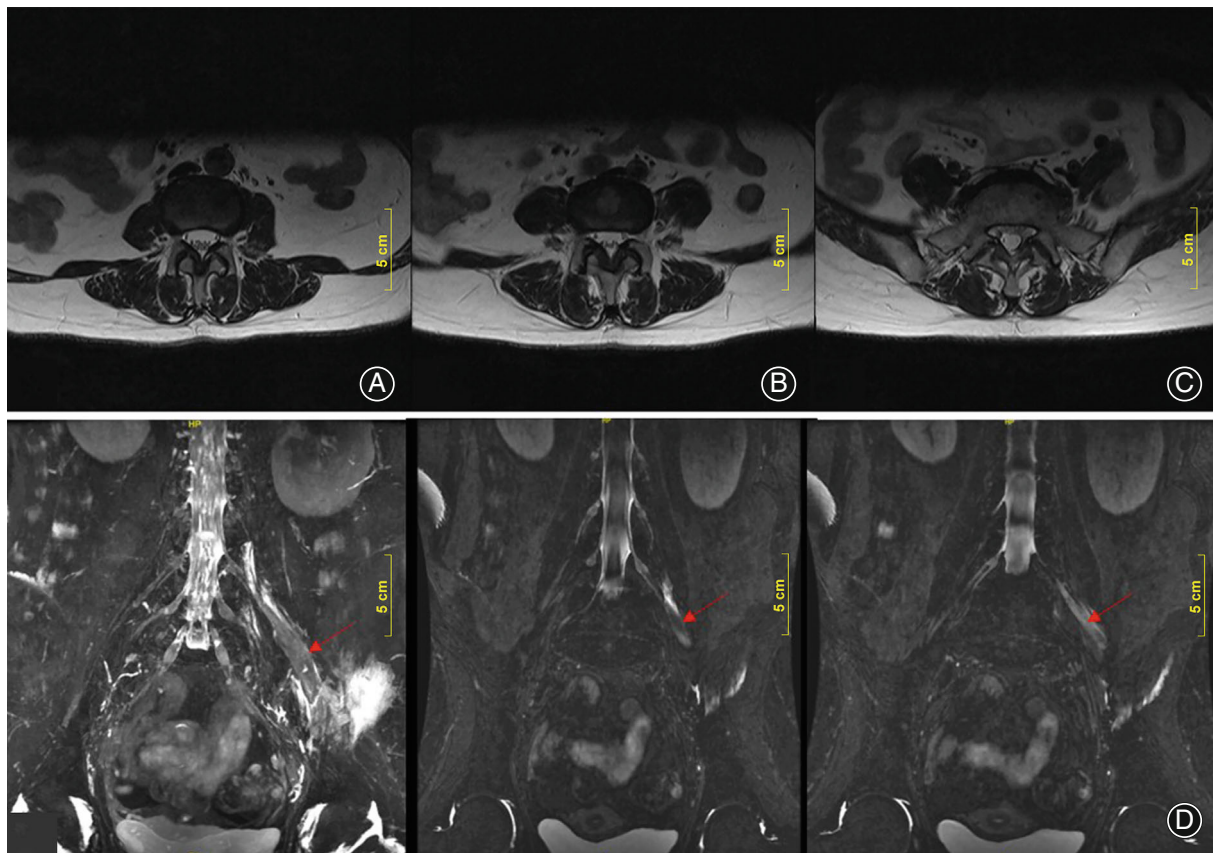


**Fig. 6** CMRI is vital for the identification of extraforaminal neuropathy. (A–C) MRI do not demonstrate obvious disc herniation and radiculopathy in the L3/4, L4/5, and L5/S1. (D) However, the extraforaminal neuropathy (idiopathic lumbosacral plexitis) was clearly shown on CMRI (red arrow).

within the schwannoma. In contrast, no annular lateral wall was observed when mimicking tumor discs on CMRI, and the signal intensity on CMRI was uniform within the mimicking tumor discs. Additionally, the signal intensity of

schwannomas was significantly higher than that of mimicking tumor discs on CMRI. Interestingly, the MRI signal intensity of mimicking tumor discs is often higher than that of parent discs.



**Fig. 7** CMRI is helpful for identifying the intradural tumor and estimating whether intradural tumor can be completely resected. (A, B) Though the intradural tumor was detected by conventional MRI, it is fairly difficult to estimate whether the tumor can be completely resected with a lesser nerve damage. (C) The CMRI not only can show the location of the tumor, but also can clearly demonstrate the spatial relationship between the tumor and cauda equina. In the patient, the cauda equina (white arrow) was not trapped within the tumor (red arrow) via the evaluation of CMRI. Therefore, the tumor was completely resected with lesser nerve damage



In addition, an intraspinal abscess also presents with a ring-like peripheral enhancement similar to mimicking tumor discs using Gd-MRI. An intraspinal abscess can also show a clear boundary between the nerve root and dura, and no annular lateral wall is observed, similar to mimicking tumor discs on CMRI. However, the signal intensity of an intraspinal abscess is higher than that of the nerve root, which is obviously different from that of mimicking tumor discs that present with hypointense and isointense signal intensities compared to the nerve root on CMRI, as shown in Case 4. In addition to this, the authors further compared the mimicking tumor discs with the extraforaminal lumbar disc the date of extraforaminal lumbar disc came from our previous article. And the MRI signal intensity of mimicking tumor discs was also higher than that of the extraforaminal lumbar disc (Supplementary Figure 1).

### Limitations

This study has some limitations. First, this was a retrospective study; thus, a selection bias was inevitable. For example, 38 patients with mimicking tumor discs were excluded. Second, this was a single-center study. A prospective, randomized, controlled, multicenter trial should be conducted in the future. Compared with conventional MRI and Gd-MRI, CMRI seems to be a better non-invasive modality for identifying mimicking tumor discs. If mimicking tumor discs can be definitively diagnosed before surgery, open surgery does not seem necessary for all patients. Minimally invasive endoscopic surgery may result in less damage, lower costs, and better therapeutic effects in some patients. Additionally, CMRI sequences present many advantages in the differential diagnosis of mimicking tumor discs and intraspinal lesions, such as intraspinal abscesses, hematomas, meningiomas, metastases, and neurinomas, as shown in Cases 3, 4, 5, and 7, respectively. Moreover, CMRI can improve the positive detection rate of extraforaminal neuropathy, such as idiopathic lumbosacral plexitis and diabetic radiculoplexus neuropathies, as shown in Case 6.

### Conclusions

In the present research, CMRI is a reliable tool for differential diagnosis of schwannomas and mimicking tumor discs. Multicenter clinical studies should be considered to further reveal the importance of CMRI for differential diagnosis of schwannomas and mimicking tumor discs.

### Conflict of Interest

The authors declare that they have no competing interests.

### Ethics Statement

This single-blind retrospective study was approved by the medical ethics committee of our institution (Review

2016, No. 001). Informed consent was obtained from all patients.

### Author Contributions

Jinghong Yuan, Jingyu Jia and Xigao Cheng contributed to the study concept and design. Zhi Du, Zhiwen Wu, Bingxue Cheng, Xi Xiong and Sikuan Zheng participated in the data acquisition and analysis. Jianhua Yin, Jingyu Jia, and Xigao Cheng evaluated the image. Jinghong Yuan, Jingyu Jia, and Xigao Cheng performed the surgery and perioperative management on the patient. Jinghong Yuan and Jingyu Jia wrote the manuscript with contributions from all co-authors. All authors contributed to the article and approved the submitted version.

### Supporting Information

Additional Supporting Information may be found in the online version of this article on the publisher's web-site:

**Supplementary Figure 1** The CMRI signal intensity of mimicking tumor discs was also higher than that of the extraforaminal lumbar disc, which may be due to vascular infiltration into the mimicking tumor discs as shown by postoperative pathology

**Supplemental Table S1** Jingyu Jia and Xigao Cheng evaluated the reliability of conventional MRI on the identification of mimicking tumor discs. McNemer test:  $p$ -value = 0.508 > 0.05; Kappa: 0.374,  $p$ -value = 0.019 < 0.05

**Supplemental Table S2** Jingyu Jia and Jianhua Yin evaluated the reliability of conventional MRI on the identification of mimicking tumor discs. McNemer test:  $p$ -value = 0.180 > 0.05; Kappa: 0.420,  $p$ -value = 0.006 < 0.05

**Supplemental Table S3** Xigao Cheng and Jianhua Yin evaluated the reliability of conventional MRI on the identification of mimicking tumor discs. McNemer test:  $p$ -value = 0.754 > 0.05; Kappa: 0.393,  $p$ -value = 0.015 < 0.05

**Supplemental Table S4** Jingyu Jia and Xigao Cheng evaluated the reliability of CMRI on the identification of mimicking tumor discs. McNemer test:  $p$ -value = 1.000 > 0.05; Kappa: 0.787,  $p$ -value < 0.001

**Supplemental Table S5** Jingyu Jia and Jianhua Yin evaluated the reliability of CMRI on the identification of mimicking tumor discs. McNemer test:  $p$ -value = 1.000 > 0.05; Kappa: 0.638,  $p$ -value < 0.001

**Supplemental Table S6** Xigao Cheng and Jianhua Yin evaluated the reliability of CMRI on the identification of mimicking tumor discs. McNemer test:  $p$ -value = 1.000 > 0.05; Kappa: 0.787,  $p$ -value < 0.001

**Supplemental Table S7** CMRI identified the mimicking tumor discs and schwannoma

**Supplemental Table S8** MRI identified the mimicking tumor discs and schwannoma

## References

1. Li K, Li Z, Geng W, Wang C, Ma J. Postdural disc herniation at L5/S1 level mimicking an extradural spinal tumor. *Eur Spine J*. 2016;25(Suppl 1):80–3.
2. Brock M, Patt S, Mayer HM. The form and structure of the extruded disc. *Spine (Phila Pa 1976)*. 1992;17(12):1457–61.
3. Montalvo Alfonso A, Mateo Sierra O, de Sagredo G, Del Corral OL, et al. Misdiagnosis of posterior sequestered lumbar disc herniation: report of three cases and review of the literature. *Spinal Cord Ser Cases*. 2018;4:61.
4. Emamian SA, Skriver EB, Henriksen L, Cortsen ME. Lumbar herniated disk mimicking neurinoma. Case report. *Acta Radiol*. 1993;34(2):127–9.
5. Ashkenazi E, Pomeranz S, Floman Y. Foraminal herniation of a lumbar disc mimicking neurinoma on CT and MR imaging. *J Spinal Disord*. 1997;10(5):448–50.
6. Hoch B, Hermann G. Migrated herniated disc mimicking a neoplasm. *Skeletal Radiol*. 2010;39(12):1245–9.
7. Ajayi O, Shoakazemi A, Tubbs RS, Moisi M, Rostad S, Newell DW. Atypical presentation of a sequestered posterolateral disc fragment. *Cureus*. 2016;8(2):e502.
8. Sharma MS, Morris JM, Pichelmann MA, Spinner RJ. L5-S1 extraforaminal intraneural disc herniation mimicking a malignant peripheral nerve sheath tumor. *Spine J*. 2012;12(12):e7–e12.
9. Levene HB, Nimmagadda A, Levi AD. An unusual case of footdrop: anterior disc herniation mimicking a nerve sheath tumor. *Neurosurgery*. 2010;66(2):E419–20. discussion E420.
10. Bakar B, Sumer MM, Cila A, Tekkok IH. An extreme lateral lumbar disc herniation mimicking L4 schwannoma. *Acta Neurol Belg*. 2009;109(2):155–8.
11. Kuo CH, Chang PY, Wu JC, Huang WC, Tu TH, Cheng H. Lumbar disc mimicking tumor. *J Neurosurg Spine*. 2014;20(6):767–8.
12. Song KJ, Kim KB, Lee KB. Sequestered thoracic disc herniation mimicking a tumoral lesion in the spinal canal – a case report. *Clin Imaging*. 2012;36(4):416–9.
13. Pillai SS. Intra-radicular disc herniation mimicking a nerve root tumor. *J Orthop Case Rep*. 2012;2(1):7–10.
14. Liu CC, Huang CT, Lin CM, Liu KN. Intradural disc herniation at L5 level mimicking an intradural spinal tumor. *Eur Spine J*. 2011;20(Suppl 2):S326–9.
15. Eksi MS, Yener U, Akakin A, Akakin D, Konya D. Posterior epidural disc herniation at L3-L4 mimicking a spinal tumor: a case report. *J Neurosurg Sci*. 2010;54(2):71–6.
16. Demirci A, Er U. A lumbar disc herniation mimicking spinal tumor with intra- and extradural components. *Spine J*. 2011;11(1):90–1.
17. Solmaz I, Onal MB, Civelek E, Sirin S, Kahraman S. Intramedullary lumbar lesion mimicking spinal cord tumor: a case of non-neoplastic intramedullary spinal cord lesion. *Eur Spine J*. 2010;19(Suppl 2):S169–73.
18. Stavrinou LC, Stranjalis G, Maratheftis N, Bouras T, Sakas DE. Cervical disc, mimicking nerve sheath tumor, with rapid spontaneous recovery: a case report. *Eur Spine J*. 2009;18(Suppl 2):176–8.
19. Saruhashi Y, Omura K, Miyamoto K, Katsuura A, Hukuda S. A migrated lumbar disc herniation simulating a dumbbell tumor. *J Spinal Disord*. 1999;12(4):307–9.
20. Dimogerontas G, Paidakakos NA, Konstantinidis E. Voluminous free disk fragment mimicking an extradural tumor. *Neurol Med Chir (Tokyo)*. 2012;52(9):656–8.
21. Bose B. Thoracic extruded disc mimicking spinal cord tumor. *Spine J*. 2003;3(1):82–6.
22. Takano M, Hikata T, Nishimura S, Kamata M. Discography aids definitive diagnosis of posterior epidural migration of lumbar disc fragments: case report and literature review. *BMC Musculoskelet Disord*. 2017;18(1):151.
23. Lee JS, Suh KT. Intradural disc herniation at L5-S1 mimicking an intradural extramedullary spinal tumor: a case report. *J Korean Med Sci*. 2006;21(4):778–80.
24. Aydin MV, Ozel S, Sen O, Erdogan B, Yildirim T. Intradural disc mimicking: a spinal tumor lesion. *Spinal Cord*. 2004;42(1):52–4.
25. Kreiner DS, Hwang SW, Easa JE, Resnick DK, Baisden JL, Bess S, et al. An evidence-based clinical guideline for the diagnosis and treatment of lumbar disc herniation with radiculopathy. *Spine J*. 2014;14(1):180–91.
26. Byun WM, Jang HW, Kim SW. Three-dimensional magnetic resonance rendering imaging of lumbosacral radiculopathy in the diagnosis of symptomatic extraforaminal disc herniation with or without foraminal extension. *Spine (Phila Pa 1976)*. 2012;37(10):840–4.
27. Shen J, Wang HY, Chen JY, Liang BL. Morphologic analysis of normal human lumbar dorsal root ganglion by 3D MR imaging. *AJNR Am J Neuroradiol*. 2006;27(10):2098–103.
28. Jia J, Ding R, Liu X, Li W, Xiong X, Wu T, et al. Coronal magnetic resonance imaging of three-dimensional fast-field echo with water-selective excitation improves the sensitivity and reliability of identification of extraforaminal lumbar disc herniation. *J Int Med Res*. 2019;47(12):6053–60.
29. Jia J, Wei Q, Wu T, He D, Cheng X. Two cases in which 3D MRI was used to differentiate between a disc mass that mimics a tumor and neurinoma. *BMC Musculoskelet Disord*. 2018;19(1):154.
30. Landis JR, Koch GG. The measurement of observer agreement for categorical data. *Biometrics*. 1977;33(1):159–74.
31. Qiangqiang W, Rui D, Shichen L, et al. Posterior epidural lumbar disc herniation: a case report. *Orthop J Chin*. 2018;26(21):2013–6.
32. Park T, Lee HJ, Kim JS, Nam K. Posterior epidural disc fragment masquerading as spinal tumor: review of the literature. *J Back Musculoskelet Rehabil*. 2018;31(4):685–91.